Natural Hazards
https://doi.org/10.1007/s11069-021-04754-1

ORIGINAL PAPER

Study of landslide geological hazard prediction method based on probability migration

Shanchao Jiang[1]

Received: 20 September 2020 / Accepted: 15 April 2021

Abstract
Based on construction of landslide displacement field detection system in Heifangtai (Lanzhou, China), landslide geological hazard prediction method based on probability migration is proposed and verified in this paper. In the hardware of landslide displacement field detection system, there are five diction points which contain 15 fiber Bragg grating (FBG) displacement sensors, and the data of detection point 1 *m1 m2* and *m3* are chosen as sample to complete data analyses. After data analyses, the future trend state of *m1* is 'S' due to that state transition probability $P_{m1}11>P_{m1}13>P_{m1}12$, *m2* is 'S' due to that $P_{m2}11>P_{m2}12>P_{m2}13$, and *m3* is 'S' due to that $P_{m3}11>P_{m3}12=P_{m3}13$. The future trend state prediction is highly consistent with the actual measured data and field observation results. These results of data analyses show that the proposed prediction method in this paper can realize effective prediction of landslide state and has important practical value for landslide prediction.

Keywords Landslide · State prediction · Field detection system · FBG · Probability migration

1 Introduction

As one of the serious natural disasters causing human death and economic loss, landslides attract more and more researchers to better understand the formation mechanism of geomorphic disasters and study the risk relationship between them and other natural disasters such as earthquakes and rainstorms (Fleurisson 2012; Santiago Martı´n 2013; Gariano et al. 2015; Tien et al. 2018). Previous studies have shown that climate change is affecting the frequency of landslides and the changes of precipitation and temperature (Gariano and Guzzetti 2016; Pavlova et al. 2017), and landslides are likely to occur on all continents, especially with the change of global climate and the intensifying of human action. Due to the severity of landslides (UNESCO 2012; Teng and Ga 2019), it is necessary to propose a practical method to detect large-scale landslides in large-scale areas, and researchers at home and abroad have done a lot of research work. Chen et al. (2012) built a collapse of geological hazard

✉ Shanchao Jiang
jiangshanchao88624@ycit.cn

[1] School of Electrical Engineering, Yancheng Institute of Technology, Yancheng 224051, China

assessment model by introducing D–S evidence theory and fuzzy comprehensive evaluation method, and the assessment model solved the uncertainty evaluation issues and had been successfully applied to Haiyuan fault zone, Ningxia. Chong (2015) applied four events to explain the necessity of establishing a unified principle for the compilation of seismic and landslide survey maps. Compared with map published by Brazilian Geological Survey (CPRM), Bragagnolo et al. (2020) presented a free and open-source add-on to the open-source Geographic Information System (GIS) GRASS software r.landslide. It can identify and pinpoint susceptible areas with better accuracy. Zhang et al. (2020) proposed a new method through combining empirical modeling with time-series Interferometric Synthetic Aperture Radar (InSAR) data to evaluate potential landslides in the Heitai River terrace of the Yellow River in central Gansu Province, China, and achieved quantify the magnitude of potential landslides. Therefore, most of the existing researches on landslide are focused on the research of image recognition algorithm (Wang et al. 2018; Yang et al. 2019; Bo et al. 2020), and the actual data on site are less. Based on the above analysis, the landslide geological hazard prediction research based on probability migration prediction is proposed through the construction of landslide displacement field detection system in this paper. After detection data analyses, the prediction research can achieve effective landslide geological hazard prediction and has important application value in protecting people's production and life safety.

2 Basic theory of Migration probability

In order to realize the effective prediction analysis of landslide state, migration probability (Morteza and Shahrbanou 2018; Wei et al. 2019) is introduced to describe the possibility of the next state and its calculation process is summarized as follows:

(1) Dividing the state of landslide.

(2) Initial probability calculation.

In the pond fish data collected, the state probability obtained from the analysis is the initial probability. When there are n states (E_1, E_2, …, E_n) and m period is observed, the state E_i appears m_i times and its probability is:

$$P_i = m_i/m. \tag{1}$$

(3) State transition probability calculation.

The probability calculation formula for calculating the state from E_i to E_j is as follows.

$$P_{ij} = m_{ij}/m. \tag{2}$$

(4) Prediction based on initial state and transition probability.

When the prediction object is in the E_i state, P_{ij} indicates the possibility of the current state E_i turning to E_j in the future. According to the maximum possibility, the prediction result chooses the largest in P_{ij} (P_{i1}, P_{i2}, …, P_{in}) as the next state of E_i.

3 Hardware construction of landslide displacement detection system

3.1 Installation location

The landslide displacement detection system is constructed to detect the slope safety of Heifangtai (Lanzhou, China), and its construction route is shown in Fig. 1.

3.2 System construction

The construction of landslide displacement detection system can be divided into site inspection, route planning, optical cable laying, sensor installation, surplus optical cable processing and fiber Bragg grating demodulator debugging, as shown in Fig. 2.

3.3 FBG displacement sensor

Fifteen FBG displacement sensors marked as *mi* ($i = 1, 2, \ldots, 15$) are used in the landslide displacement detection system, and each detection point shown in Fig. 1 installs three FBG displacement sensors. Measuring range of the FBG displacement sensor is 0–300 mm with 0.5% sensitivity, installation direction in each detection point is 0°/45°/90°, and its install effect diagram is shown in Fig. 3.

3.4 FBG demodulator

FBG demodulator (including wireless module) is mainly used to realize the modulation and demodulation of photoelectric signal, and its field installation effect diagram is shown

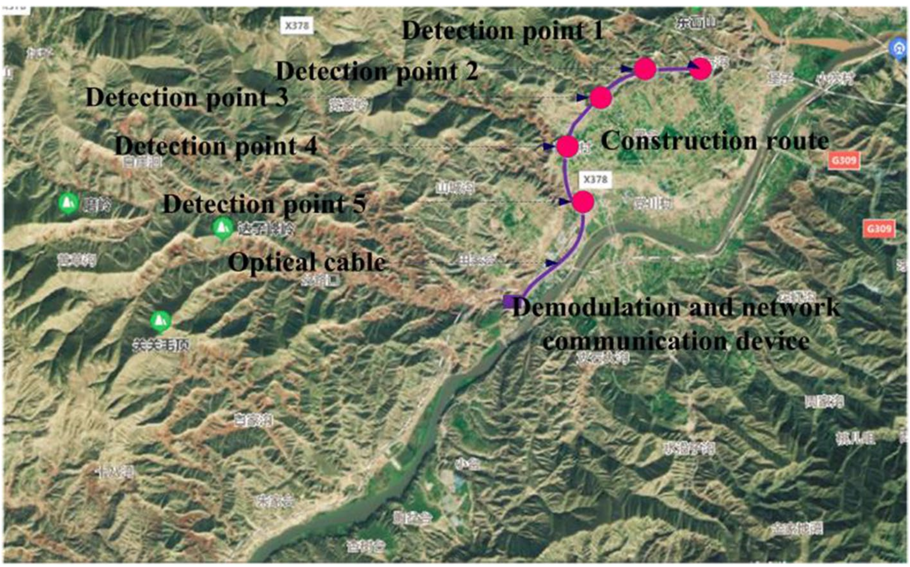

Fig. 1 Detection system construction route

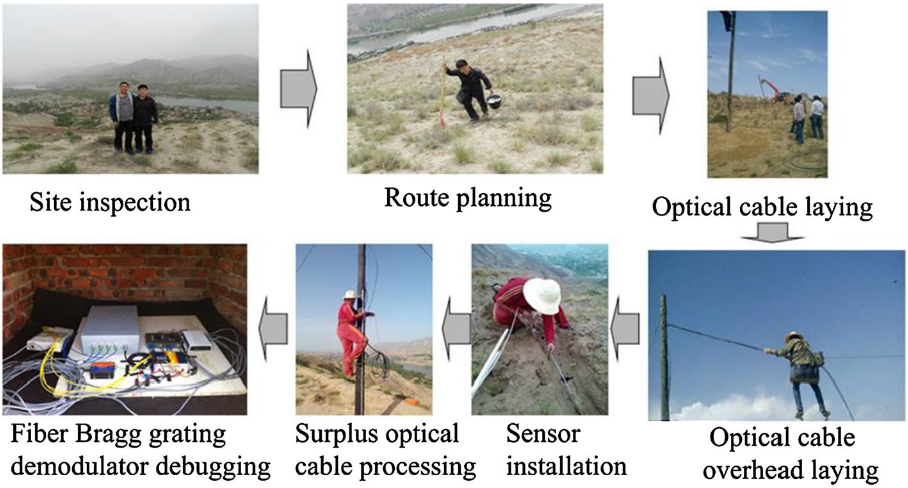

Fig. 2 Schematic diagram of detection system installation process

Fig. 3 Install effect diagram

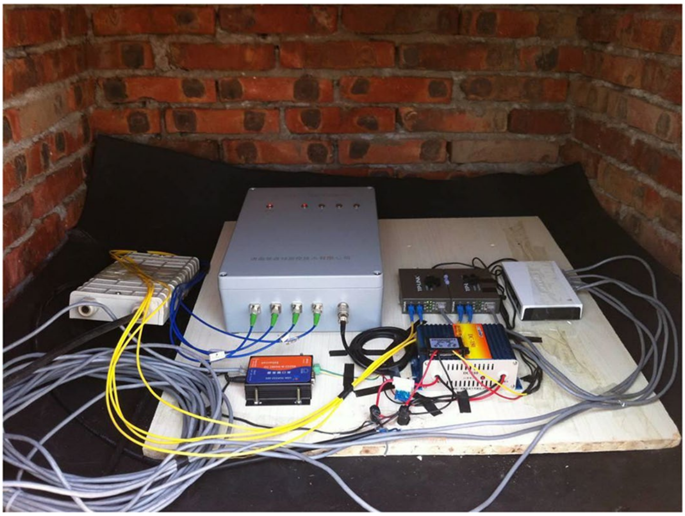

Fig. 4 Install effect diagram of FBG demodulator

in Fig. 4. The black insulation sponge in Fig. 4 is mainly used for moisture proof in summer and heat preservation in winter.

4 Software of landslide displacement detection system

The software of landslide displacement detection system can mainly realize the following functions: (1) real-time monitoring and storage of sensor data; (2) automatic conversion of current displacement, relative displacement and absolute displacement; (3) real-time curve display of daily displacement; (4) historical displacement query, statistics and historical curve display; and (5) parameter setting and maintenance. The main interface and historical data query interface of the software are shown in Fig. 5.

5 Data analyses

The data of detection point 1 shown in Fig. 1 are chosen as sample to complete data analyses. Detection data of three FBG displacement sensors marked as *m1*, *m2* and *m3* in detection point 1 are shown in Fig. 6.

At the beginning of sampling sequence, data of detection point 1 exhibit considerable variation as shown in Fig. 1. The considerable variation caused by the rainy season at Heifangtai. After the rainy season, Heifangtai enters the dry season and the displacement data changes little which is consistent with the data change trend of detection point 1. In the dry season, the fluctuation of detection data may be caused by creep of Heifangtai loess. In order to complete and display data analyses, the displacement at the beginning of the sampling sequence is taken as the initial displacement value and data analyses selection sampling interval is 500. For more detailed data analysis, smaller values can be selected for selection sampling interval. Furthermore, the original displacement data of data analyses are shown in Table 1.

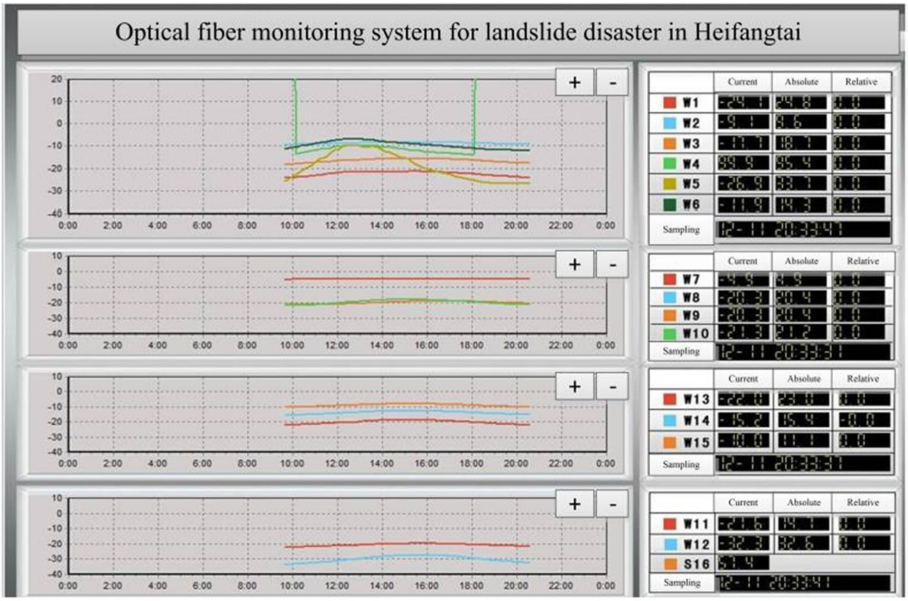

(a) Main interface

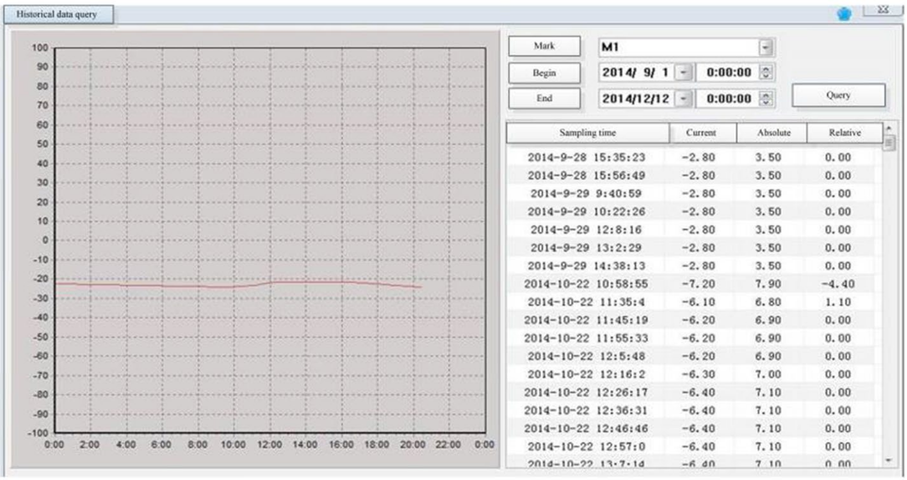

(b) Historical data query interface

Fig. 5 Software interface

Firstly, at the beginning of data analyses, the state of landslide is divided into safe (‘S’), transition (‘T’) and dangerous (‘D’), and the judgment threshold between different states of landslide can vary according to the state level, and here, its value is 5 mm. In other words, the landslide belongs to the safe state if the displacement change is less than 5 mm, and it is the dangerous state if the displacement change is more than 10 mm, and it is the transitional state if the displacement change is more than 5 mm and

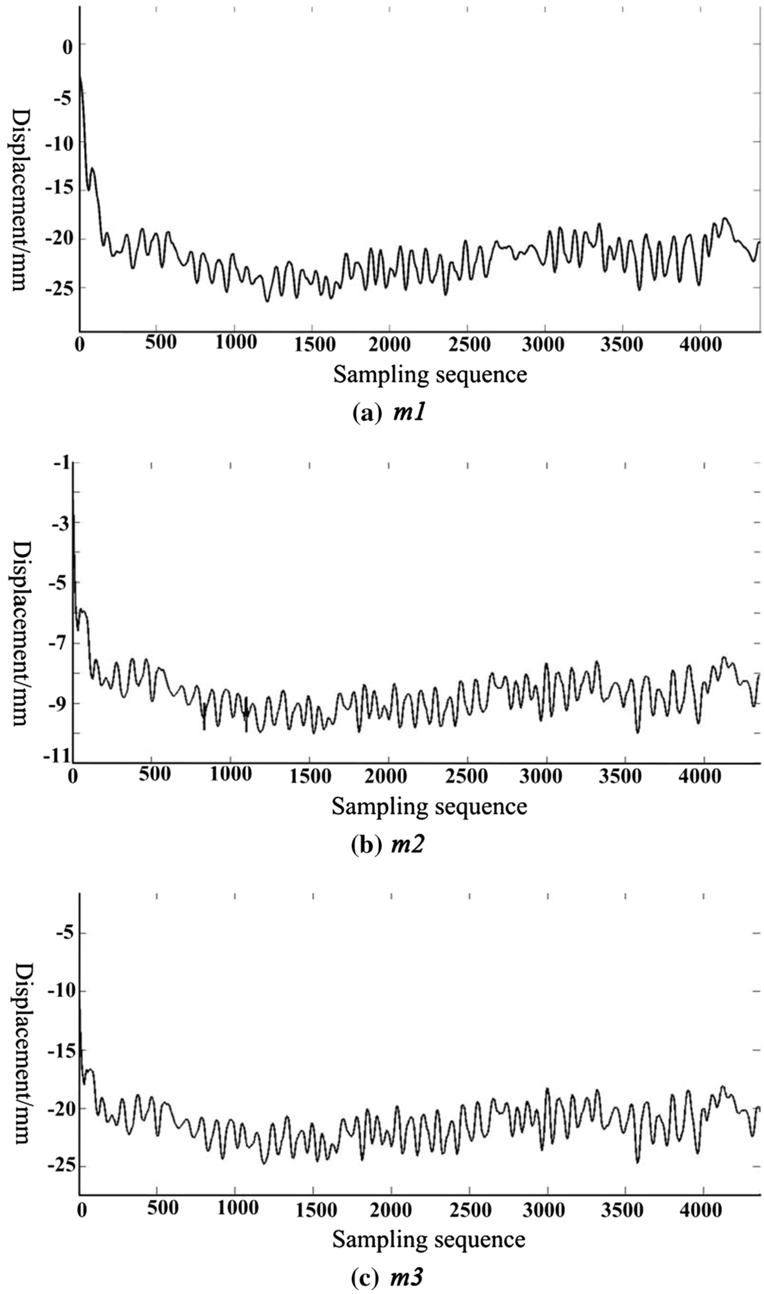

Fig. 6 Data of detection point 1

Table 1 The original displacement data of data analyses

Sampling sequence	m1/mm	m2/mm	m3/mm
0	−2.8	−1.2	−3.6
500	−19.6	−8.6	−16.6
1000	−21.8	−9	−17.2
1500	−23.5	−9.2	−17.3
2000	−23.1	−10.2	−20
2500	−21.3	−10.3	−20.2
3000	−19.9	−8	−14.1
3500	−21	−8.9	−17
4000	−24	−8.1	−14.5

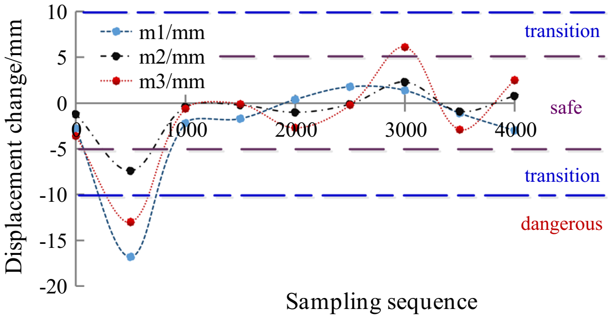

Fig. 7 State dividing

less than 10 mm. Secondly, the initial probability calculation is completed as shown in Fig. 7.

Thirdly, state transition probability of m_1, m_2 and m_3 is calculated and displayed as follows:

$$\mathrm{P}_{m_1} = \begin{array}{c c} & \begin{array}{ccc} S & T & D \end{array} \\ \begin{array}{c} S \\ T \\ D \end{array} & \begin{bmatrix} 6/7 & 0 & 1/7 \\ 0 & 0 & 0 \\ 1 & 0 & 0 \end{bmatrix} \end{array}, \mathrm{P}_{m_2} = \begin{array}{c c} & \begin{array}{ccc} S & T & D \end{array} \\ \begin{array}{c} S \\ T \\ D \end{array} & \begin{bmatrix} 6/7 & 1/7 & 0 \\ 1 & 0 & 0 \\ 0 & 0 & 0 \end{bmatrix} \end{array}, \mathrm{P}_{m_3} = \begin{array}{c c} & \begin{array}{ccc} S & T & D \end{array} \\ \begin{array}{c} S \\ T \\ D \end{array} & \begin{bmatrix} 2/3 & 1/6 & 1/6 \\ 1 & 0 & 0 \\ 1 & 0 & 0 \end{bmatrix} \end{array}. \quad (3)$$

Finally, the prediction of landslide trend state is completed according to the final state of the current measurement and state transition probability. As shown in Fig. 7, the final states of m_1, m_2 and m_3 are all in 'S.' So, the future trend state of *m1* is 'S' due to that $P_{m1}11 > P_{m1}13 > P_{m1}12$, *m2* is 'S' due to that $P_{m2}11 > P_{m2}12 > P_{m2}13$, and *m3* is 'S' due to that $P_{m3}11 > P_{m3}12 = P_{m3}13$. Based on the above data analyses, there is no danger of landslide at detection point 1 which is highly consistent with the actual measured data in Fig. 6 and field observation results. Therefore, the study of landslide geological hazard prediction and analysis based on probability migration proposed in this paper can not only realize the effective prediction of landslide state, but also have the advantages of less analysis data and less influence by loess creep of the measured point compared with the analysis of measured data.

6 Conclusions

In order to achieve the prediction of landslide state, landslide geological hazard prediction method based on probability migration is studied in this paper. To verify the effectiveness of the landslide geological hazard prediction method, one landslide displacement detection system on Heifangtai (Lanzhou, China) is constructed to verify the practicability of probability migration prediction, and the landslide displacement detection system consists of two parts: hardware and software. In the hardware, 15 FBG displacement sensors marked as *mi* ($i = 1, 2, \ldots, 15$) are used and each detection point installs three FBG displacement sensors, and the data of detection point 1 *m1*, *m2* and *m3* are chosen as sample to complete data analyses. At the beginning of data analyses, the state of landslide is divided into safe ('S'), transition ('T') and dangerous ('D'). After data analyses, the final states of m_1, m_2 and m_3 are all in 'S' according to the state transition probability of m_1, m_2 and m_3, and the future trend state prediction results are highly consistent with the actual measured data and field observation results. Based on the above analyses, the prediction method introduced in this paper can not only realize the prediction of landslide state, but also have the advantages of less analysis data and less influence by loess creep of the measured point compared with the analysis of measured data. So, prediction method of this paper has important practical value for landslide prediction.

Acknowledgements This work was co-supported by National Natural Science Foundation of China (No. 61803325), the Natural Science Foundation of Jiangsu Province (No. BK20181049), the Natural Science Foundation of the Jiangsu Higher Education Institutions of China (No. 18KJB510046), Jiangsu Province Six Talent Peaks Project (NO. XYDXX-103), R&D Demonstration Project of Jiangsu Provincial Emergency Management Department (No. YJGL-YF-2020-13), New Generation Information Technology Innovation Project of Science and Technology Development Center of Ministry of Education (No. 2019ITA01024) and China Scholarship Council (No. 202008320064).

Author's contributions Shanchao Jiang conceived of the study, participated in its design and coordination and helped to draft the manuscript.

Availability of data and material Not applicable.

Code availability Not applicable.

Declarations

Conflict of interest The author declares no conflict of interest in preparing this article.

References

Bo Yu, Chen F, Chong Xu (2020) Landslide detection based on contour-based deep learning framework in case of national scale of Nepal in 2015. Comput Geosci 135:104388

Bragagnolo L, da Silva RV, Grzybowski JMV (2020) Landslide susceptibility mapping with r.landslide: a free open-source GIS-integrated tool based on artificial neural networks. Environ Modell Softw 123: 104565

Chen L, Wang W, Zhang W (2012) Risk evaluation of regional collapses geological hazard based on D-S Evidence theory-a case study of Haiyuan active fault belt in Ningxia Province. Energy Proced 16:371–376

Chong Xu (2015) Preparation of earthquake-triggered landslide inventory maps using remote sensing and GIS technologies: principles and case studies. Geosci Front 6:825–836

Fleurisson J-A (2012) Slope design and implementation in open pit mines geological and geomechanical approach. Proced Eng 46:27–38

Gariano SL, Guzzetti F (2016) Landslides in a changing climate. Earth Sci Rev 162:227–252

Gariano S, Petrucci O, Guzzetti F (2015) Changes in the occurrence of rainfallinduced landslides in Calabria, southern Italy, in the 20th century. Nat Hazards Earth Syst Sci 15:2313–2330

Martín S, Uzkeda H, Poblet J, Bulnes M, Rubio R (2013) Construction of accurate geological cross-sections along trenches, cliffs and mountain slopes using photogrammetry. Comput Geosci 51:90–100

Morteza J, Shahrbanou S (2018) Stochastic discontinuum analysis of hydrocarbon migration probability around an unlined rock cavern based on the discrete fracture networks. Tunn Undergr Space Technol 81:41–54

Pavlova I, Makarigakis A, Depret T, Jomelli V (2017) Global overview of the geological hazard exposure and disaster risk awareness at world heritage sites. J Cult Herit 28:151–157

Teng W, Ga Z (2019) Failure behavior of soil-rock mixture slopes based on centrifuge model test. J Mt Sci 16(8):1928–1942

Tien BD, Shahabi H, Shirzadi A, Chapi K, Alizadeh M, Chen W, Mohammadi A, Ahmad B, Panahi M, Hong H (2018) Landslide detection and susceptibility mapping by AIRSAR data using support vector machine and index of entropy models in Cameron Highlands. Malaysia Remote Sens 10:1527

UNESCO (2012) Operational guidelines for the implementation of the World Heritage convention. UNESCO World Heritage Centre, World Heritage Centre, Paris

Wang S, Yang B, Zhou Yi (2018) Three-dimensional information extraction from GaoFen-1 satellite images for landslide monitoring. Geomorphology 309:77–85

Wei Y, Zhan M-l, Huang Q-f (2019) Erosion probability model of base-soil particle migration into a granular filter under local flow. Int J Sedim Res 34:455–460

Yang Y, Song S, Yue F (2019) Superpixel-based automatic image recognition for landslide deformation areas. Eng Geol 259:105166

Zhang Y, Meng XM, Dijkstra TA (2020) Forecasting the magnitude of potential landslides based on InSAR techniques. Remote Sens Environ 241:111738